



PERGAMON

International Journal of Multiphase Flow 27 (2001) 929–946

International Journal of
**Multiphase
Flow**

www.elsevier.com/locate/ijmulflow

Gas holdup in bubble columns at elevated pressure via computed tomography

Abdenour Kemoun, Boon Cheng Ong, Puneet Gupta, Muthanna H. Al-Dahhan^{*},
Milorad P. Dudukovic

*Chemical Reaction Engineering Laboratory, Department of Chemical Engineering, Campus Box 1198, 1 Brookings Drive,
Washington University St. Louis, MO 63130-4899, USA*

Abstract

Gas holdup in a pressurized bubble column (pressures from 0.1 to 0.7 MPa) was studied in a laboratory scale vessel (diameter 0.162 m) with air–water system over a range of superficial gas velocities (0.02–0.18 m/s) using non-invasive γ -ray based Computed Tomography (CT). It was found that the cross-sectional average gas holdup increases with pressure, as well as with superficial gas velocity. At all operating conditions, the azimuthally averaged radial gas holdup profiles exhibit a characteristic shape with greater gas holdup in the column center than by the walls. It is also observed that with an increase in pressure, the transition to churn-turbulent regime characterized by the change of the radial gas holdup profile from relatively flat to almost parabolic, is delayed to higher superficial gas velocities. The average cross-sectional gas holdup at each operating condition was compared with predictions of existing correlations and large discrepancies in predictions (as high as 300%) were found. © 2001 Elsevier Science Ltd. All rights reserved.

Keywords: Gas–liquid flow; Bubble column; Computed tomography; High pressure; High superficial gas velocity

1. Introduction

Bubble column reactors are vertical cylindrical columns, with or without internal heat exchanger tubes, where a gas is contacted with a liquid or slurry for production of chemicals and other products. Two-phase bubble columns as well as three-phase slurry bubble columns of various configurations have gained considerable attention in the chemical process industry due to their use in a number of processes, such as, Fischer–Tropsch synthesis, liquid phase methanol synthesis, wet oxidation of heavily polluted effluent, hydrogenation of heavy oils, etc. For

^{*} Corresponding author. Tel.: +1-314-935-7187; fax: +1-314-935-7211.
E-mail address: muthanna@wuche.wustl.edu (M.H. Al-Dahhan).

commercially important applications, bubble column reactors are usually operated at conditions of elevated pressures (Deckwer, 1992; Joshi et al., 1998). However, research on details of bubble column hydrodynamics has primarily been limited to studies performed at atmospheric conditions. For lack of anything better, design and scale-up of such bubble column reactors for commercial applications invariably utilize information from studies performed at atmospheric conditions, which has often been reported to result in either over-design or poor estimates of bubble column performance. This raises a question as to whether one can rely solely on the database established at atmospheric pressure.

Bubble columns have been extensively studied for the last several decades, with almost all the studies on bubble column hydrodynamics discussing the importance of gas holdup, defined as the volume fraction of the gas phase in the reactor, and how it affects liquid recirculation and back-mixing. Kölbel et al. (1961) reported that gas holdup in a bubble column with a porous plate distributor was not affected by pressure in the range 0.1–1.6 MPa when the superficial gas velocity, evaluated at the pressure in the column, was less than 0.03 m/s. Deckwer et al. (1980) measured gas holdup in a slurry bubble column with a porous plate distributor containing fine particles at pressures up to 1.1 MPa and with superficial gas velocity below 0.04 m/s. They also found no significant effect of pressure on gas holdup in that range of operating variables. Idogawa et al. (1986) observed that the behavior of bubbles depends closely on the type of gas distributor, and this dependence weakens as the pressure is increased. The effect vanished above 10 MPa. In a later study, Idogawa et al. (1987) reported that pressure had no effect on bubble diameter in bubble columns with gas superficial velocity in the range of 0.005–0.05 m/s. Jiang et al. (1995), studying a column of 0.0508 m in diameter at superficial gas velocities of up to 1 m/s and in the pressure range from 0.1 to 21 MPa, observed that as pressure increases, the bubble size decreases, and the bubble size distribution becomes narrower. Many other studies have been reported in the literature which discuss the effect of pressure and superficial gas velocity (Hammer et al., 1984; Oyevaar and Westerterp, 1989; Oyevaar et al., 1989; Kojima et al., 1991; Shollenberger et al., 1995; Adkins et al., 1996; Shollenberger et al., 1997; Kojima et al., 1997; Lin et al., 1998; Luo et al., 1999).

The main aim of this study is to investigate the effect of pressure on gas holdup and its distribution over a range of superficial gas velocities using a non-intrusive technique, Computed Tomography (CT). A γ -ray based CT has been developed (Kumar et al., 1995) for imaging phase holdup distribution in two-phase flow systems such as bubble columns and other multiphase reactors. The CT measurements were performed using an encapsulated γ -ray radiation source (Cs^{137}) and a fan beam arrangement of detectors. The details of the hardware and software have been described elsewhere (Kumar, 1994; Kumar et al., 1995, 1997) and will not be repeated here. Instead, the obtained experimental measurements are discussed. The average cross-sectional holdup is compared to values obtained from various correlations reported in the literature.

2. Experimental setup

Fig. 1 displays the flowsheet for the high-pressure system used in this study. The system is designed to handle a high flow rate of air at a pressure of up to 1.5 MPa. The bubble column is made of a stainless steel tube with inner diameter 0.162 m (6.359") and height 2.5 m (8.2'). A transparent glass window is situated at the top of the column and is named 'blue eye'. This

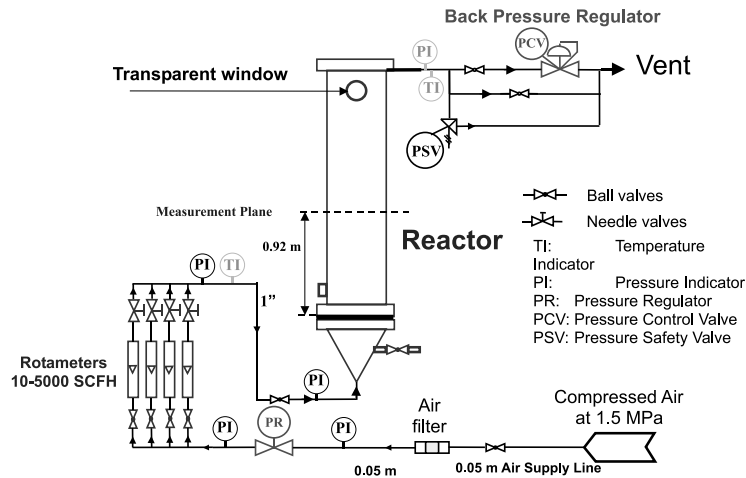


Fig. 1. Flowsheet for high pressure bubble column facility.

window allows viewing the system before starting the CT scan. The gas was dispersed into the column through a perforated plate distributor. The distributor used in this study has 61 holes each of 0.0004 m diameter, providing an open area of 0.04%. The holes are arranged in three concentric circles with 20 holes on each circle and one at the center of the distributor plate. The increment in radius between the circles on which holes are centered is 0.015 m. This particular distributor was used because a significant amount of data for gas holdup distribution and liquid velocity is available for this distributor from our previous studies conducted at atmospheric pressure conditions. In this study, tomographic scans were conducted at three pressures ($P = 0.1, 0.3, 0.7$ MPa) and four superficial gas velocities ($U_G = 0.02, 0.05, 0.12, 0.18$ m/s).

Air was used as the gas phase and was filtered before being continuously introduced into the system at ambient temperature ($T = 20^\circ\text{C}$), while tap water served as the liquid medium with no net flow of the liquid (operation was batchwise with respect to the liquid). The gas flow rate was maintained at the desired values with the aid of a set of needle valves and rotameters. After exiting the bubble column, the gas passes through a backpressure regulator, which is used to control the pressure in the column. It is then discharged into the atmosphere through a vent. Two pressure safety valves are mounted both at the top and bottom of the column to prevent accidental over-pressurization. The height of the two-phase gas–liquid mixture in all experiments was maintained between 1.8 and 2.0 m from the distributor and therefore, the initial height of the liquid varied depending on the operating condition.

As already mentioned, in this study time-averaged cross-sectional gas holdup distribution was measured using the γ -ray scanner and associated tomography reconstruction algorithms developed in Chemical Reaction Engineering Laboratory (CREL) and discussed by Kumar et al. (1995, 1997). The CREL scanner is a versatile instrument that enables the quantification of the time-averaged holdup distribution for two-phase flows under a wide range of operating conditions. The fan beam configuration of the scanner consists of an array of NaI detectors of 0.05 m in diameter (5 detectors were used in this study), and an encapsulated 100 mCi Cs^{137} source located opposite to the center of the array of detectors. During each scan, the source-detectors assembly is rotated

360° around the test section to obtain multiple projection measurements. The total time of a complete 360° scan is approximately 2 h. The tomographic scans can be acquired at different axial positions, which allows for the quantification of the effects of operating conditions on the axial variation of gas holdup distribution. In this study however, the axial variation of gas holdup was not considered, and measurements were conducted at only one axial location about 0.92 m from the distributor, which is in the fully developed flow region of the column.

3. Results and discussions

3.1. Cross-sectional gas holdup distribution

Fig. 2 shows the time-averaged cross-sectional distribution of the gas holdup in the bubble column at different pressures and at different superficial gas velocities studied (results for only a few conditions are shown). For example, Fig. 2(a) shows the pixel map for $P=0.3$ MPa, and $U_G=0.05, 0.12$ and 0.18 m/s. A gradual variation in the color shades for the gas holdup from the column center to the wall indicates a change in gas holdup value. The plots confirm that gas holdup increases with pressure and superficial gas velocities. Visual observations of the column in the vicinity of the wall via the blue eye revealed much smaller bubbles when the pressure was increased. This could be explained in terms of a decrease in the rate of coalescence and a corresponding increase in bubble breakup rates at pressurized conditions. Hence, gas holdup increases as pressure increases, and the transition to churn-turbulent regime gets delayed to higher superficial gas velocities, which is characterized by the relatively flatter azimuthally averaged radial gas holdup profiles.

3.2. Radial gas holdup distribution

From Fig. 2, one can see that in the long time-averaged sense, the cross-sectional gas holdup distributions in bubble columns are close to being axisymmetric. Therefore, one is justified in representing the cross-sectional distribution by azimuthal averaging of the two-dimensional data as represented by Eq. (1).

$$\varepsilon_G(r) = \frac{1}{2\pi} \int_0^{2\pi} \varepsilon_G(r, \theta) d\theta, \quad (1)$$

where $\varepsilon_G(r)$ represents the radial gas holdup profile.

Figs. 3–6 display, respectively, the azimuthally averaged radial gas holdup distributions at different superficial gas velocity as a function of operating pressure. These plots were obtained from the CT measured holdup distribution in a cross-section of the column 0.92 m above the distributor. This axial location was chosen for this study as it was far away from the distributor and the gas–liquid interface in the freeboard region. Our past experience indicates that at L/D ratio of 6 or above (where L is the total height of the dispersed two-phase mixture; and D is the diameter of the column), the holdup profiles in the well-developed region (region excluding the entrance and exit zones) are relatively invariant to axial position (Kumar, 1994). The profiles at atmospheric conditions indeed conform to the results previously obtained by Kumar (1994).

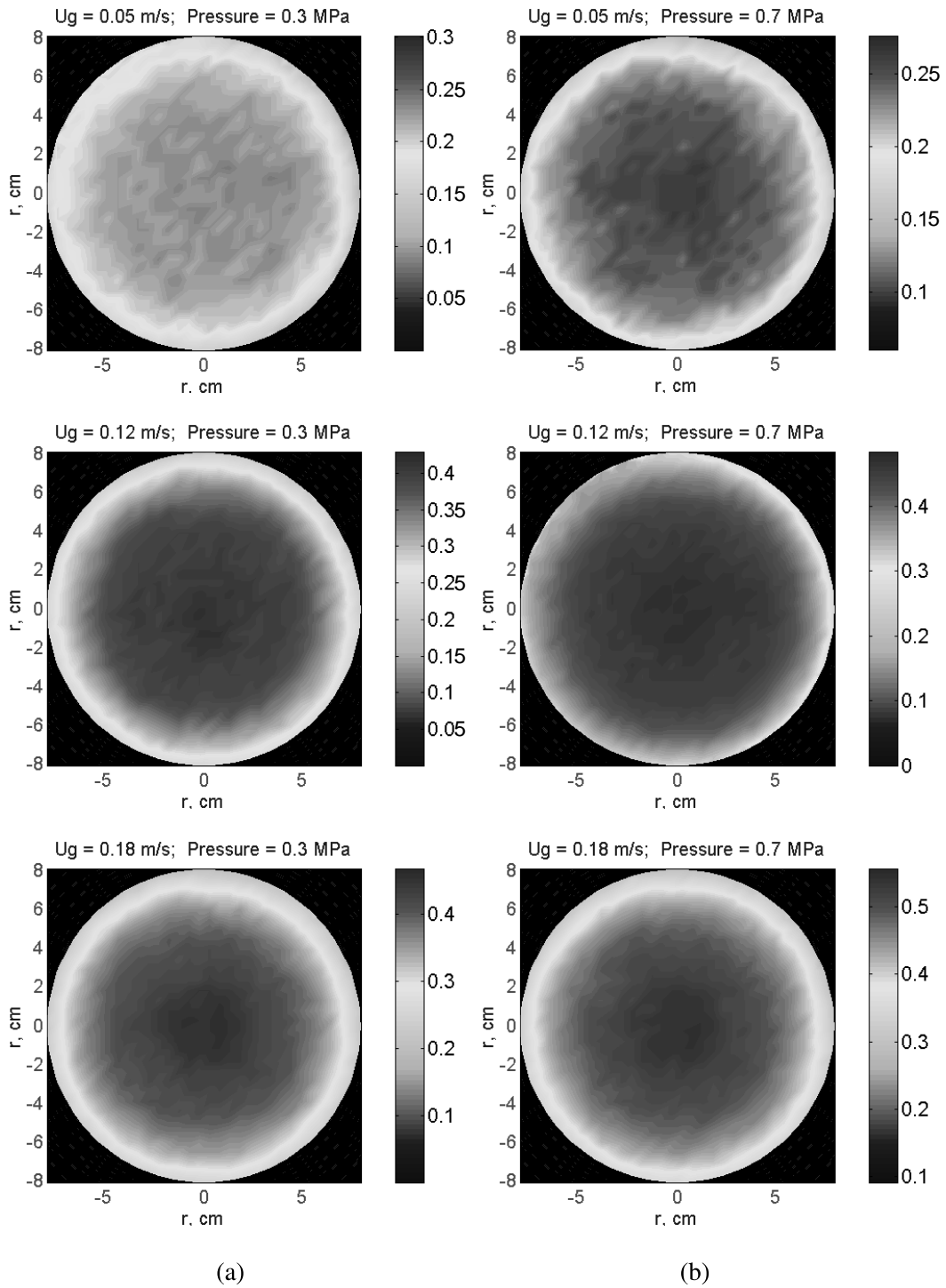


Fig. 2. Cross-sectional gas holdup distribution at (a) $P = 0.3$ MPa and (b) $P = 0.7$ MPa for $U_g = 0.05, 0.12$ and 0.18 m/s.

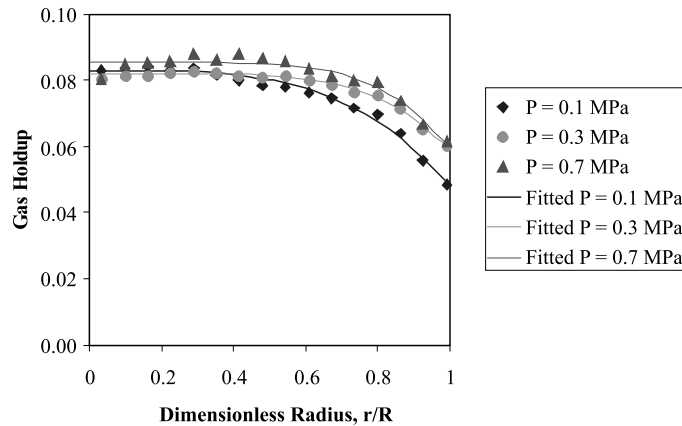


Fig. 3. Radial gas holdup distribution as a function of pressure for $U_g = 0.02$ m/s.

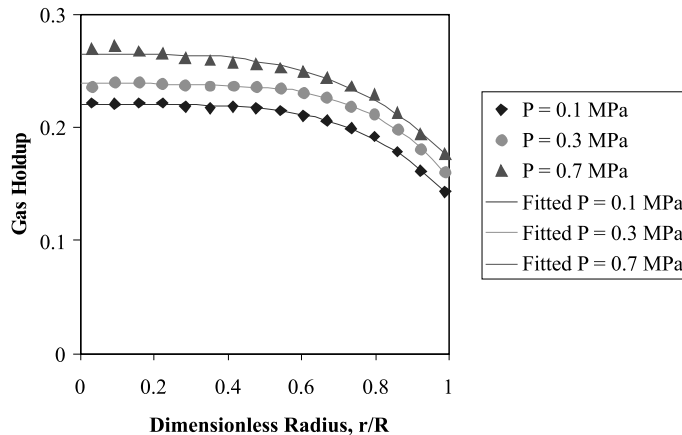


Fig. 4. Radial gas holdup distribution as a function of pressure for $U_g = 0.05$ m/s.

From these figures it is apparent that the differences in the radial gas holdup profiles, as a result of increase in pressure, become more pronounced with an increase in the superficial gas velocity.

Fig. 7 displays the results obtained by Shollenberger et al. (1995) at atmospheric conditions. The trend in gas holdup profiles at atmospheric pressure with increasing superficial gas velocities observed in our laboratory Figs. 3–6 agrees well with their results. However, the gas holdup obtained in this study is slightly higher than that observed by Shollenberger et al. (1995). For example, at a velocity of 0.1176 m/s, the gas holdup value at the center of the column observed by Shollenberger et al. (1995) is about 0.22 (Fig. 7), whereas in our case, a gas holdup value of about 0.28 is obtained (Fig. 5) at the column center. Such discrepancies might be due to the differences in the type of distributor and the column diameter used in these two studies. Shollenberger et al. (1995) used a bubble cap distributor, whereas in this study a non-uniform perforated plate was used as the gas distributor. It is also possible that the observed differences were a result of the different tap water used in the two laboratories.

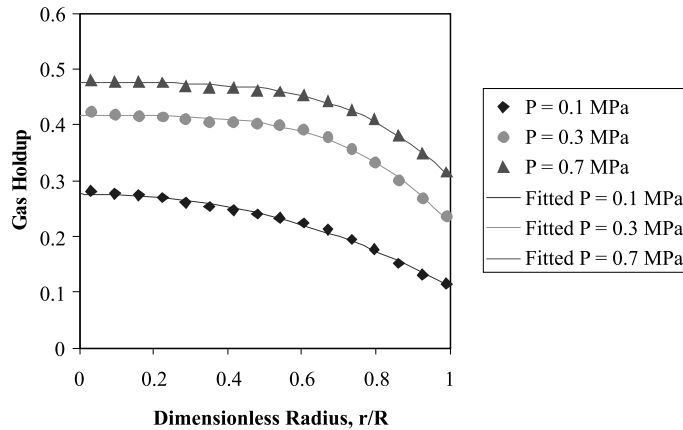


Fig. 5. Radial gas holdup distribution as a function of pressure for $U_g = 0.12$ m/s.

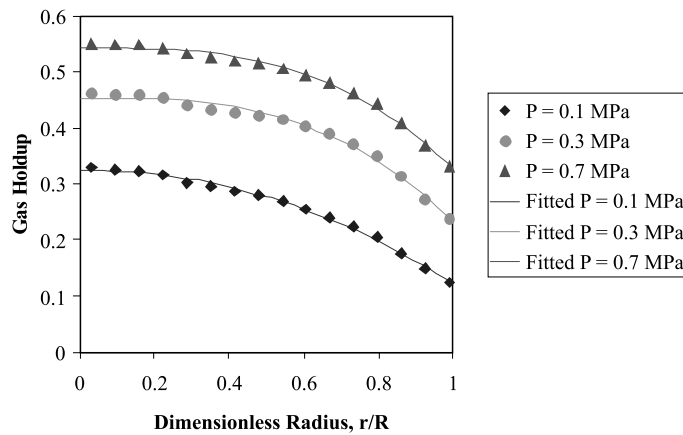


Fig. 6. Radial gas holdup distribution as a function of pressure for $U_g = 0.18$ m/s.

From Figs. 3–6 it is evident that gas holdup increases both with pressure, and with superficial gas velocity in agreement with the experimental data reported in the literature (Idogawa et al., 1986; Jiang et al., 1995; Kojima et al., 1991; Kojima et al., 1997; Lin et al., 1998; Oyevaar and Westerterp, 1989; Luo et al., 1999). At a velocity of 0.12 m/s (Fig. 5), the radial gas holdup profile at atmospheric pressure is parabolic in nature, indicating churn turbulent flow, whereas at higher pressure, the profile is flatter. This can be seen more clearly from Table 1, which shows the three parameters of the power law expression (Eq. (2)) used to fit the radial gas holdup profiles.

$$\varepsilon_G(r) = \tilde{\varepsilon}_G \left(\frac{m+2}{m} \right) \left[1 - c \left(\frac{r}{R} \right)^m \right], \tag{2}$$

where m is the exponent; c allows the possibility of non-zero gas holdup close to the wall; R the column radius; and $\tilde{\varepsilon}_G$ is related to the cross-sectional average gas holdup, $\bar{\varepsilon}_G$, by Eq. (3).

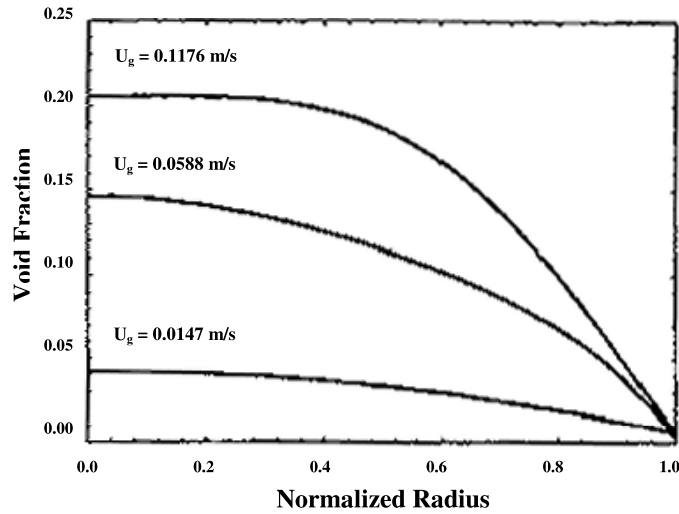


Fig. 7. Radial distribution of gas holdup as a function of superficial gas velocity for 0.19 m air–water column with bubble cap distributor (Shollenberger et al., 1995).

Table 1
Parameters of the fitted radial holdup profile

| P (MPa) | U_G (m/s) | $\tilde{\varepsilon}_G$ | m | c |
|-----------|-------------|-------------------------|-------|-------|
| 0.1 | 0.02 | 0.053 | 3.633 | 0.422 |
| | 0.05 | 0.151 | 4.372 | 0.368 |
| | 0.12 | 0.145 | 2.228 | 0.605 |
| | 0.18 | 0.165 | 2.068 | 0.622 |
| 0.3 | 0.02 | 0.059 | 5.133 | 0.283 |
| | 0.05 | 0.168 | 4.792 | 0.345 |
| | 0.12 | 0.272 | 3.765 | 0.466 |
| | 0.18 | 0.270 | 2.955 | 0.487 |
| 0.7 | 0.02 | 0.062 | 5.424 | 0.307 |
| | 0.05 | 0.170 | 3.557 | 0.346 |
| | 0.12 | 0.315 | 3.937 | 0.356 |
| | 0.18 | 0.326 | 2.997 | 0.396 |

$$\bar{\varepsilon}_G = \tilde{\varepsilon}_G \left(\frac{m + 2 - 2c}{m} \right). \quad (3)$$

This expression has been frequently used to represent the radial gas holdup distribution. Parameter m is indicative of the magnitude of the gradient of the radial gas holdup profile. If m is approximately equal to 2, then the profile is parabolic. As m increases the profile becomes flatter. One can see from Table 1 that as the pressure increases, for a given superficial gas velocity, the value of m goes up indicating that the radial gas holdup profile gets flatter except for $U_G = 0.05$ m/s which is in the transition regime at atmospheric pressure. The radial gas holdup profiles fitted to

the expression in Eq. 2 for each operating condition have also been plotted in Figs. 3–6, respectively.

Adkins et al. (1996), who used a different γ -ray tomography system, report slightly different observations as can be seen in Fig. 8, which displays their radial gas holdup distribution at $U_G = 0.1$ m/s. In a 0.48 m ID and 3 m tall column, they found that the gas holdup profile is parabolic at a pressure of 0.394 MPa and gas superficial velocity of 0.1 m/s. In their study, the sparger was a 0.15 m diameter ring formed from 0.011 m ID stainless steel tubing. There were 12 holes equidistantly distributed on the ring, each of 0.00318 m in diameter. Hence, the discrepancies might be due to the type of distributor and size of column used or difference in water quality.

3.3. Cross-sectional average gas holdup

The cross-sectional average gas holdup is calculated via Eq. (3) by averaging the radial gas holdup profiles obtained from Eq. (1).

$$\bar{\varepsilon}_g = \frac{2}{R^2} \int_0^R r \varepsilon_g(r) dr. \quad (4)$$

The cross-sectional average gas holdup can be taken as a good estimate of the overall gas holdup (Kumar, 1994). Fig. 9 displays the cross-sectional average gas holdup as a function of pressure at different superficial gas velocities.

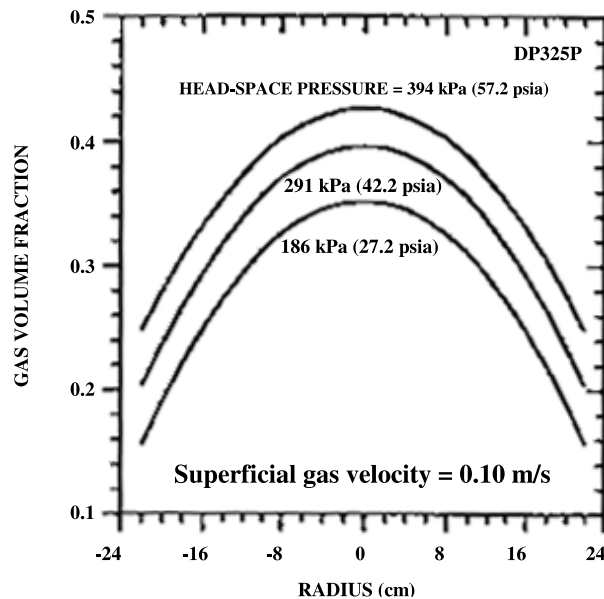


Fig. 8. Radial distribution of gas holdup as a function of pressure for $U_g = 0.1$ m/s (taken from Shollenberger et al., 1996).

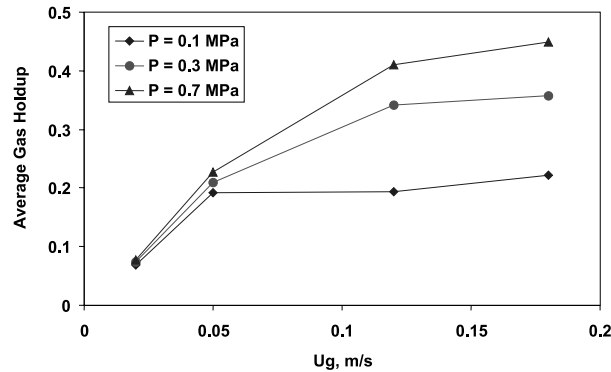


Fig. 9. Cross-sectional average gas holdup as a function of superficial gas velocity at different pressures.

Fig. 9 further confirms that gas holdup increases with pressure, except at low superficial gas velocities (below and up to 0.05 m/s) where it is rather insensitive to pressure. At atmospheric pressure, the cross-sectional average gas holdup seems almost constant after certain superficial gas velocity is reached as indicated by Fig. 9. This leveling-off effect seems to occur at higher gas velocities at higher pressures. These observations have also been reported in the literature (Kölbel et al., 1961; Deckwer et al., 1980). Wilkinson and van Dierendonck (1990) explained the effect of pressure on gas holdup in terms of the Kelvin–Helmholtz stability analysis. They concluded from their analysis that pressure mainly affects the stability of large bubbles, which tend to break due to growth of surface instabilities. Since at low superficial gas velocities the large bubble holdup is negligible, pressure does not significantly influence gas holdup.

Table 2 compares the average gas holdup measurements obtained by Adkins et al. (1996) and Shollenberger et al. (1997) with gas holdup values obtained from this study. One can see that there is significant deviation in the values of cross-sectional average gas holdup obtained in these studies. The cause of the discrepancies is unknown. Neither the fluid (tap water) nor the distributor or column diameter was matched. Moreover, the data at $U_G = 0.05$ m/s superficial gas velocity is probably in the transition regime at atmospheric pressure conditions, which could possibly explain the observed differences. However, it is known that gas holdup increases with

Table 2
Comparison of results from this study with literature data

| Study | Column ID (m) | U_G (m/s) | Pressure (MPa) | $\bar{\epsilon}_G$ |
|-----------------------------|---------------|-------------|----------------|--------------------|
| Shollenberger et al. (1997) | 0.19 | 0.0147 | 0.1 | 0.024 |
| Present | 0.162 | 0.02 | 0.1 | 0.069 |
| Shollenberger et al. (1997) | 0.19 | 0.0588 | 0.1 | 0.082 |
| Present | 0.162 | 0.05 | 0.1 | 0.191 |
| Shollenberger et al. (1997) | 0.19 | 0.1176 | 0.1 | 0.126 |
| Present | 0.162 | 0.12 | 0.1 | 0.193 |
| Adkins et al. (1996) | 0.48 | 0.125 | 0.141 | 0.211 |
| Present | 0.162 | 0.12 | 0.3 | 0.342 |
| Adkins et al. (1996) | 0.48 | 0.066 | 0.299 | 0.185 |
| Present | 0.162 | 0.05 | 0.3 | 0.210 |

increasing column diameter (Akita and Yoshida, 1973), and one should expect a higher holdup in the studies of Adkins et al. (1996) and Shollenberger et al. (1997) as compared to our experimental data, which is acquired in a smaller diameter vessel. The only other possible reason for this observed trend could be the effect of the water quality, or more significantly, the effect of the rigidity of the column support structure, which could explain the higher holdups observed in our studies due to stabilized bubbly flow even at significantly high superficial gas velocities.

3.4. Comparison with various correlations in the literature

Numerous correlations for overall gas holdup in bubble columns have been reported and those that seem applicable to the conditions investigated in this study (based on the pressure range, gas flow rates and column diameter) are summarized in Table 3. Since Kumar (1994) has shown that the cross-sectional average holdup measured at heights above the distributor larger than 4–5 column diameters is in close agreement with the overall gas holdup in the column, the cross-sectional average holdup determined in this study was compared to the prediction for overall gas holdup obtained from the reported correlations. Fig. 10 shows the predictions for the overall gas holdup as a function of superficial gas velocity based on various correlations at $P=0.1$ MPa. It can be concluded that the correlation of Idogawa et al. (1985) agrees closely with our experimental data followed by correlations of Hikita et al. (1980); Luo et al. (1999); Wilkinson et al. (1992); Akita and Yoshida (1973). At $U_G=0.05$ m/s, the above mentioned predictions deviate from the observed holdup (refer to Table 4 which gives an error analysis of the various correlations against experimental data obtained in this study).

Since the superficial gas velocity of 0.05 m/s is close to the transition velocity at $P=0.1$ MPa that changes bubbly flow into churn turbulent flow, and the precise value of the transition velocity is a function of the non-measurable water quality, it is possible that the deviation between data and correlation predictions at $U_G=0.05$ m/s is caused by the fact that the correlations predict the holdup in one flow regime while the data reflect the other flow regime. It is evident from Fig. 10 that the experimental holdup value at $U_G=0.05$ m/s at $P=0.1$ MPa is considerably higher than the value predicted by any of the correlations indicating perhaps a different flow regime during our experiment than observed in the data used to develop the correlations.

In the same manner, Figs. 11 and 12 display the plots for the cross-sectional average gas holdup as a function of superficial gas velocity at $P=0.3$ and 0.7 MPa, respectively. Among the correlations reported in Table 3 those of Idogawa et al. (1985), Idogawa et al. (1987), Wilkinson et al. (1992) and Luo et al. (1999) were developed by considering high-pressure data also. As evident from Figs. 11 and 12, the gas holdup predictions based on the correlation of Hammer et al. (1984) are in good agreement with the observed cross-sectional gas holdup, which yields an average deviation of about 12% (for 0.3 MPa) to 17% (for 0.7 MPa), except for low superficial gas velocities where the correlation is in error of 21%. The correlations of Wilkinson et al. (1992) and Idogawa et al. (1987) also predict holdup values in reasonable agreement with experimental observations, and have average deviation of about 18% for all conditions, except at low superficial gas velocities where these correlations are in error of about 40%. The correlation of Kojima et al. (1997) gives reasonable estimate of holdup at all pressures investigated in this study. However, it has limited applicability to superficial gas velocities less than 0.1 m/s (Kojima, 1999).

Table 3
Correlations for gas holdup

| References | Gas–liquid system | Apparatus | Conditions | Correlations |
|---------------------------------------|---|---|---|--|
| Akita and Yoshida (1973) ^a | He/CO ₂ /O ₂ /air–H ₂ O/glycol/methanol/ CCl ₄ /Na ₂ SO ₃ /NaCl | $D = 0.152, 0.301,$ 0.6 m Sparger (5.0 mm) | $P = 0.1$ MPa, $T = 283–313$, K $U_G = 0.5–40$ cm/s | $\frac{\bar{\epsilon}_G}{(1 - \bar{\epsilon}_G)^4} = 0.2 \left(\frac{gD^2 \rho_L}{\gamma_L} \right)^{0.125} \left(\frac{gD^3}{v_L} \right)^{0.083} \frac{U_G}{(gD)^{0.5}}$ |
| Hikita et al. (1981) ^a | H ₂ /CO ₂ /CH ₄ /C ₃ H ₈ /H ₂ + N ₂ /air–H ₂ O/sucrose/methanol/ <i>n</i> -butanol/aniline/ <i>i</i> -butanol/NaCl/ Na ₂ SO ₄ /CaCl ₂ /MgCl ₂ /AlCl ₃ /KCl/ K ₂ SO ₄ /K ₃ PO ₄ /KNO ₃ | $D = 0.10$ m Nozzle (1.1 cm) | $P = 0.1$ MPa, $H/$ $D = 15, U_G = 4.2–38$ cm/s | $\bar{\epsilon}_G = 0.672 f \left(\frac{U_G \mu_L}{\gamma_L} \right)^{0.578} \left(\frac{\mu_L^4 g}{\rho_L \gamma_L^3} \right)^{-0.131}$ $\left(\frac{\rho_G}{\rho_L} \right)^{0.062} \left(\frac{\mu_G}{\mu_L} \right)^{0.107}$ where $f = \begin{cases} 1.0 & \text{for-electrolyte solution,} \\ 10^{0.0414I} & \text{for } 0 < I < 1.0 \text{ kg ion/m}^3, \\ 1.1 & \text{for } I > 1.0 \text{ kg ion/m}^3. \end{cases}$ |
| Hammar et al. (1984) ^a | N ₂ /He/Ar/CO ₂ /Air–H ₂ O/ organic liquids–glas ballotini | $D = 0.106, 0.2$ m Annuli or stars spargers (17–40 holes of 0.5, 1 or 2 mm ID) | $P = 0.1$ MPa, $T = 293–363$, K $U_G = 0.5–13$ cm/s | $\frac{\bar{\epsilon}_G}{1 - \bar{\epsilon}_G} = 0.4 \left(\frac{U_G \mu_L}{\gamma_L} \right)^{0.87} \left(\frac{\mu_L^4 g}{\rho_L \gamma_L^3} \right)^{-0.27} \left(\frac{\rho_G}{\rho_L} \right)^{0.17}$ |
| Idogawa et al. (1985) ^{a,b} | Air–H ₂ O | $D = 0.05$ m Porous plate (2, 100 μm) Capillary tubes (1, 3, 5 mm) Perforated plate (19 holes of 1 mm) | $P = 0.1–15$ MPa, $H/$ $D = 16.6, U_G = 0.5–5$ cm/s, $T = 288–293$ K | $\frac{\bar{\epsilon}_G}{1 - \bar{\epsilon}_G} = 1.44 U_G^{0.58} \rho_G^{0.12} \sigma_L^{-0.16 \exp(-P)}$ |
| Reilly et al. (1986) ^a | He/Ar/air–H ₂ O/solvent/ trichloroethylene–glass beads | $D = 0.3$ m Perforated plate (293 holes, 1.5 mm) Single sparger Multiorifice sparger (13.4 mm) | $P = 0.1$ MPa, $T = 283–323$ K, $U_G = 0.4–40$ cm/s | $\bar{\epsilon}_G = 296 U_G^{0.44} \rho_L^{-0.98} \rho_G^{0.19} \gamma_L^{-0.16} + 0.009$ |
| Idogawa et al. (1987) ^{a,b} | H ₂ /He/air–H ₂ O/methanol/ ethanol/acetone/aqueous alcohol solution | $D = 0.05$ m Perforated plate (19 holes of 1 mm) | $P = 0.1–5$ MPa, $T = 284–293$ K, $H/D = 16.6,$ $U_G = 0.5–5$ cm/s | $\frac{\bar{\epsilon}_G}{1 - \bar{\epsilon}_G} = 0.059 U_G^{0.8} \rho_G^{0.17} \left(\frac{\sigma_L}{\gamma_L} \right)^{-0.22 \exp(-P)}$ |
| Wilkinson et al. (1992) ^a | N ₂ –H ₂ O/ <i>n</i> -heptane/ mono-ethylene glycol | $D = 0.158, 0.23$ m Sparger ring (4 holes of 7 mm) | $P = 0.1–2.0$ MPa, $H = 1.2$ m, $U_G = 0–60$ cm/s | $U_G < U_{\text{TRANS}} \quad \bar{\epsilon}_G = \frac{U_G}{U_{\text{S.B.}}},$ $U_G > U_{\text{TRANS}} \quad \bar{\epsilon}_G = \frac{U_{\text{TRANS}}}{U_{\text{S.B.}}} + \frac{U_G - U_{\text{TRANS}}}{U_{\text{L.B.}}},$ where $\frac{U_{\text{TRANS}}}{U_{\text{S.B.}}} = 0.5 \exp(-193 \rho_G^{-0.61} \mu_L^{0.5} \gamma_L^{0.11}),$ $\frac{\mu_L U_{\text{S.B.}}}{\gamma_L} = 2.25 \left(\frac{\gamma_L^3 \rho_L}{g \mu_L^4} \right)^{-0.273} \left(\frac{\rho_L}{\rho_G} \right)^{0.03},$ |

| | | | | |
|---|--|---|---|--|
| | | | | $\frac{\mu_L U_{L.B.}}{\gamma_L} = \frac{\mu_L U_{S.B.}}{\gamma_L}$ $+ 2.4 \left[\frac{\mu_L (U_G - U_{TRANS})}{\gamma_L} \right]^{0.757} \left(\frac{\gamma_L^3 \rho_L}{g \mu_L^4} \right)^{-0.077} \left(\frac{\rho_L}{\rho_G} \right)^{0.077}$ $\bar{\varepsilon}_G = \left\{ \begin{array}{l} 129 \left(\frac{U_G \mu_L}{\gamma_L} \right)^{0.99} \left(\frac{\mu_L^4 g}{\rho_L \gamma_L^3} \right)^{-0.123} \left(\frac{\rho_G}{\rho_L} \right)^{0.187} \\ \left(\frac{\mu_G}{\mu_L} \right)^{0.343} \left(\frac{d}{D} \right)^{-0.089} \end{array} \right\}$ |
| Sotelo et al. (1994) ^{a,c} | Air/CO ₂ -H ₂ O/ethanol/saccharose/glycerin | D = 0.04, 0.08 m Porous gas diffusers (30, 65, 150 μm) | P = 0.1 MPa, H = 1.5–2.0 m, U _G = 0–20 cm/s | |
| Krishna and Ellenberger (1996) ^a | Air/He/Ar/SF ₆ -H ₂ O/paraffin oil/separan/tetradecane | D = 0.1, 0.174, 0.19, 0.38 and 0.63 m, Spider sparger, Sintered glass plate (mean pore size of 150–200 μm), Polyacrylate sieve plate (2.5 mm ID), Sintered bronze plate (mean pore size of 50 μm) | P = 0.1 MPa, U _G = 0.1–85 cm/s | $U_G < U_{TRANS} \quad \bar{\varepsilon}_G = \varepsilon_b,$ $U_G > U_{TRANS} \quad \bar{\varepsilon}_G = \varepsilon_B + \varepsilon_{TRANS}(1 - \varepsilon_B),$ <p>where</p> $\varepsilon_B = 0.268 \frac{(U_G - U_{TRANS})^{0.58}}{D^{0.18}},$ $U_{TRANS} = V_{SMALL} \varepsilon_{TRANS} (1 - \varepsilon_{TRANS}),$ $V_{SMALL} = \frac{\gamma_L^{0.12}}{2.84 \rho_G^{0.04}},$ $\varepsilon_{TRANS} = 0.59(3.85)^{1.5} \sqrt{\frac{\rho_G^{0.96} \gamma_L^{0.12}}{\rho_L}}$ |
| Kojima et al. (1997) ^{a,d} | Air-H ₂ O/aqueous buffered solution/aqueous enzyme solution | D = 0.045 m Nozzle (1.38, 2.1, 2.9, 4.03 mm) | P = 0.1–1.1 MPa, T = 290–300 K, H/ D = 20–26.7, U _G = 0.005–0.15 cm/s | $\bar{\varepsilon}_G = 1.18 U_G^{0.679} \left(\frac{\gamma_L}{\gamma_{L,0}} \right)^{-0.546}$ $\times \exp \left[1.27 \times 10^{-4} \left(\frac{\rho_L Q^2}{d_o^3 \gamma_L} \right) \left(\frac{P}{P_0} \right) \right]$ |
| Luo et al. (1999) ^a | N ₂ -Paratherm NF-alumina particles | D = 0.102 m Perforated plate (120 squared-pitched holes of 1.5 mm ID) | P = 0.1–5.6 MPa, T = 298–351 K, U _G = up to 45 cm/s | $\frac{\bar{\varepsilon}_G}{1 - \bar{\varepsilon}_G} = \frac{2.9 \left(\frac{U_G^4 \rho_G}{\gamma_L g} \right)^\alpha \left(\frac{\rho_G}{\rho_{SL}} \right)^\beta}{[\cosh(Mo_{SL}^{0.054})]^{0.41}},$ <p>where</p> $Mo_{SL} = \frac{(\zeta \mu_L)^4 g}{\rho_{SL} \gamma_L^3},$ $\alpha = 0.21 Mo_{SL}^{0.0079}; \beta = 0.096 Mo_{SL}^{-0.011}; \rho_{SL} = \rho_L; \zeta = 1$ |

^a γ_L is the liquid surface tension in N/m; $\gamma_{L,0}$ is the surface tension of water at 20°C in N/m; ν_L is the liquid kinematic viscosity in m²/s; ρ_G is the gas density in kg/m³; and ρ_L is the liquid density in kg/m³.

^b σ_L is the liquid surface tension in mN/m.

^c d is the inner diameter of single nozzle in m.

^d d_o is the orifice ID in mm; P_0 is the standard atmospheric pressure; and Q is the volumetric flow rate of gas under the condition in the bubble column in m³/s.

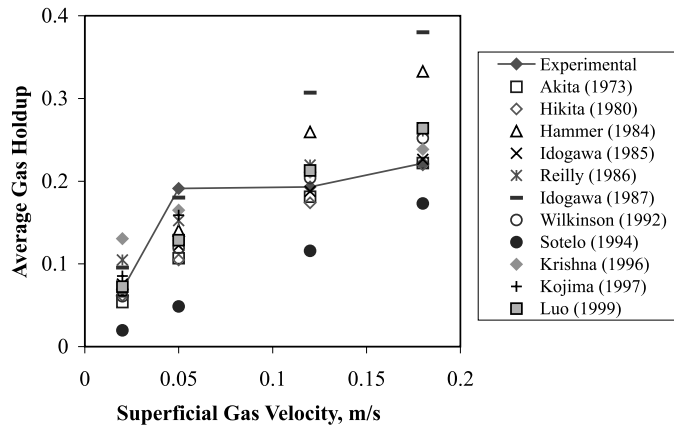


Fig. 10. Cross-sectional average gas holdup as a function of superficial gas velocity at atmospheric pressure.

4. Conclusions

The gas holdup and its cross-sectional distribution were measured at elevated pressures up to 0.7 MPa using γ -ray CT. These measurements indicate that gas holdup increases very slightly with pressure at low superficial gas velocities of less than 0.05 m/s and then increases significantly with system pressure at higher superficial gas velocities owing to a decrease in the stable bubble size, which results in an increase in the number of small bubbles. As mentioned earlier, this reduction in bubble size with increasing pressure is usually attributed to a decreased rate of coalescence of bubbles and an enhanced breakup of large (unstable) bubbles, which gets promoted under pressurized conditions. It was also shown that the radial gas holdup distribution tends to become relatively flatter at a higher pressure as compared to that at atmospheric pressure. For example, at atmospheric pressure and $U_G = 0.12$ m/s, the gradient of the radial gas holdup distribution is steeper, indicating churn-turbulent flow conditions; whereas at higher pressures of 0.3 and 0.7 MPa, the gradient is not so steep which indicates a stabilized bubble regime.

The cross-sectional average gas holdup was calculated using the collected data and compared with various correlations found in the literature. The main findings are:

- At atmospheric pressure, the correlation of Idogawa et al. (1985) was in the best agreement with our experimental data except for $U_G = 0.05$ m/s. This operating condition is near the transition point, and the correlation and data may not belong to the same flow regime.
- At higher pressures and over the entire superficial gas velocity range investigated in this study, the correlation of Hammer et al. (1984) gives the best prediction of our gas holdup data (average error of 12–17%) followed by Wilkinson et al. (1992; average error of 14–18%) and Idogawa et al. (1987; average error of 18–20%).
- At higher pressures and high superficial gas velocity ($U_G > 0.1$ m/s), in addition to the correlations of Idogawa et al. (1987), and Hammer et al. (1984), the correlation of Krishna and Ellenberger (1996) and Luo et al. (1999) also seem to provide reasonable predictions of the measured gas holdup.

Table 4
Error analysis for different correlations (percent error is reported)^a

| U_G (m/s) | Akita and Yoshida (1973) | Hikita (1980) | Hammer (1984) | Idogawa (1985) | Reilly (1986) | Idogawa (1987) | Wilkinson (1992) | Sotelo (1994) | Krishna and Ellenbergera (1996) | Kojima (1997) | Luo (1999) |
|----------------------|--------------------------------|------------------|------------------|-------------------|------------------|-------------------|---------------------|------------------|---------------------------------------|------------------|---------------|
| <i>P</i> = 0.1 (MPa) | | | | | | | | | | | |
| 0.02 | 22.1 | 10.6 | 0.7 | 9.5 | 51.5 | 38.3 | 11.9 | 71.6 | 88.7 | 23.5 | 5.0 |
| 0.05 | 44.1 | 45.1 | 26.4 | 36.0 | 20.3 | 5.7 | 37.6 | 74.5 | 13.7 | 16.8 | 32.7 |
| 0.12 | 6.2 | 9.9 | 34.4 | 2.7 | 13.7 | 59.0 | 5.6 | 40.0 | 9.3 | – | 10.3 |
| 0.18 | 0.05 | 0.8 | 50.1 | 2.1 | 17.6 | 71.4 | 13.8 | 22.0 | 7.6 | – | 19.0 |
| Average | 18.1 | 16.6 | 27.9 | 12.6 | 25.8 | 43.6 | 17.2 | 52.0 | 29.8 | 20.2 | 16.8 |
| <i>P</i> = 0.3 (MPa) | | | | | | | | | | | |
| 0.02 | – | 10.4 | 10.6 | 28.4 | 72.1 | 53.2 | 6.6 | 67.3 | 199.62 | 17.2 | 32.8 |
| 0.05 | – | 46.5 | 21.5 | 28.0 | 11.6 | 0.1 | 26.6 | 71.5 | 13.7 | 17.7 | 19.0 |
| 0.12 | – | 45.6 | 13.3 | 33.3 | 21.6 | 1.7 | 25.4 | 58.5 | 16.2 | – | 20.2 |
| 0.18 | – | 34.2 | 4.9 | 23.9 | 10.8 | 18.8 | 12.9 | 40.6 | 12.5 | – | 7.1 |
| Average | | 34.2 | 12.6 | 28.4 | 29.0 | 18.5 | 17.9 | 59.5 | 60.5 | 17.5 | 19.8 |
| <i>P</i> = 0.7 (MPa) | | | | | | | | | | | |
| 0.02 | – | 9.6 | 20.7 | 56.3 | 91.3 | 66.3 | 7.3 | 63.3 | 330.3 | 18.9 | 59.1 |
| 0.05 | – | 48.0 | 18.5 | 16.9 | 4.9 | 3.0 | 15.0 | 69.2 | 45.9 | 9.5 | 8.2 |
| 0.12 | – | 52.1 | 20.0 | 31.8 | 23.4 | 6.9 | 21.3 | 59.3 | 6.25 | – | 20.4 |
| 0.18 | – | 44.6 | 8.6 | 26.6 | 16.7 | 2.7 | 13.3 | 44.5 | 9.1 | – | 12.8 |
| Average | – | 38.6 | 17.0 | 32.9 | 34.1 | 19.7 | 14.2 | 59.1 | 97.9 | 14.2 | 25.1 |

^a

$$\text{Absolute error} = \left| \frac{\text{Measured value} - \text{Predicated value}}{\text{Measured Value}} \right| \times 100\%.$$

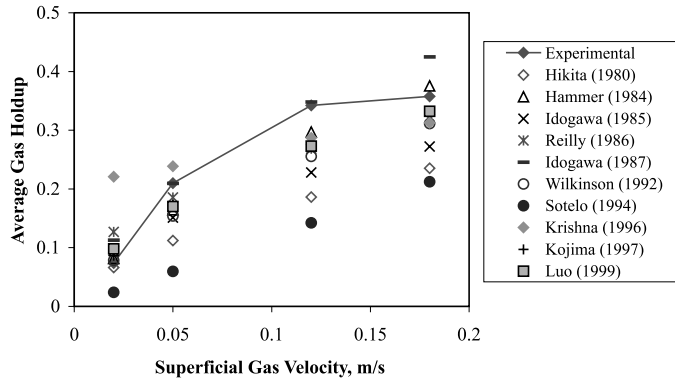


Fig. 11. Cross-sectional average gas holdup as a function of superficial gas velocity at $P = 0.3$ MPa.

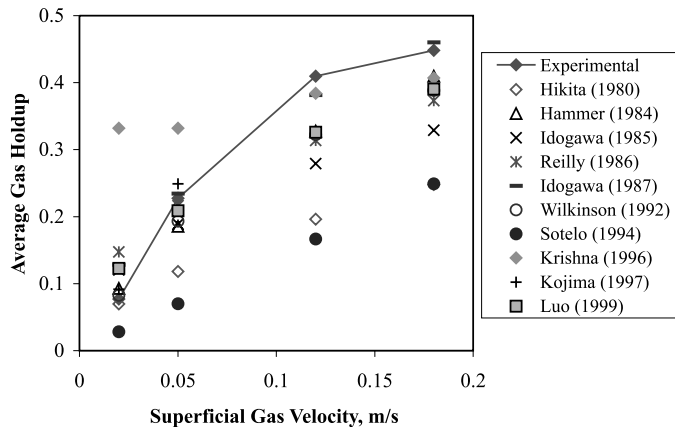


Fig. 12. Cross-sectional average gas holdup as a function of superficial gas velocity at $P = 0.7$ MPa.

In spite of several correlations giving reasonable predictions, we did not find any correlation that consistently predicted our experimental data, which indicates the need for better characterization of the levels of liquid recirculation and turbulence which are needed for development of a more fundamentally based model for prediction of gas holdups. Such work is currently underway.

Acknowledgements

Department of Energy grant (DE-FG2295PC-95212) through the University Coal Research Program (UCR), Exxon Research and Engineering support, and Department of Energy grant (DE-FC-2s2-95 PC 95051) through Air Products and Chemicals, Inc. are gratefully acknowledged.

References

- Adkins, D.R., Shollenberger, K.A., O'Hern, T.J., Torczynski, J.R., 1996. Pressure effects on bubble column flow characteristics. In: ANS Proceedings, 1996 National Heat Transfer Conference, Technical Sessions sponsored by Thermal Hydraulics Division American Nuclear Society, 3–6 August, vol. 9, pp. 318–325.
- Akita, K., Yoshida, F., 1973. Gas holdup and volumetric mass transfer coefficient in bubble columns. *Ind. Eng. Chem. Process Des. Dev.* 12, 76–80.
- Deckwer, W.-D., 1992. *Bubble Column Reactors*. Wiley, New York.
- Deckwer, W.D., Louisi, Y., Zaidi, A., Ralek, M., 1980. Hydrodynamic properties of the Fischer–Tropsch slurry process. *Ind. Eng. Chem. Process Des. Dev.* 19, 699–708.
- Hammer, H., Schrog, H., Hektor, K., Schönau, K., Küsters, W., Soemarno, A., Sahabi, U., Napp, W., 1984. New subfunctions in hydrodynamics, heat and mass transfer for gas/liquid and gas/liquid/solid chemical and biochemical reactors. *Front. Chem. Reac. Eng.* 464.
- Hikita, H., Asai, S., Tanigawa, K., Segawa, K., Kitao, M., 1980. Gas holdup in bubble columns. *Chem. Eng. J.* 20, 59–67.
- Idogawa, K., Ikeda, K., Fukuda, T., Morooka, S., 1985. Effect of gas and liquid properties on the behavior of bubbles in a bubble column under high pressure. *Kag. Kog. Ronb.* 11, 432.
- Idogawa, K., Ikeda, K., Fukuda, T., Morooka, S., 1986. Behavior of bubbles of the air–water system in a column under high pressure. *Int. Chem. Eng.* 26, 468–474.
- Idogawa, K., Ikeda, K., Fukuda, T., Morooka, S., 1987. Effect of gas and liquid properties on the behavior of bubbles in a column under high pressure. *Int. Chem. Eng.* 27, 93–99.
- Jiang, P., Lin, T.-J., Luo, X., Fan, L.-S., 1995. Flow visualization of high pressure (21 MPa) bubble column: bubble characteristics. *Trans. IChemE* 73, 269–274.
- Joshi, J.B., Veera, U., Parasu Prasad, Ch.V., Phanikumar, D.V., Deshpande, N.S., Thakre, S.S., Thorat, B.N., 1998. Gas holdup structure in bubble column reactors. *PINSA* 64, 441–567.
- Kojima, H., 1999. Personal communication.
- Kojima, H., Jun, S., Hideyuki, S., 1997. Effect of pressure on volumetric mass transfer coefficient and gas holdup in bubble column. *Chem. Eng. Sci.* 52, 4111–4116.
- Kojima, H., Okumura, B., Nakamura, A., 1991. Effect of pressure on gas holdup in a bubble column and a slurry bubble column. *J. Chem. Eng. Jpn.* 24, 115–117.
- Kölbel, H., Borchers, E., Langemann, H., 1961. Großenverteilung der Gasblasen in Blasensäulen Teil I: Einflüsse von Flüssigkeitsviscosität und Säuleninnendruck. *Chemie-Ing.-Technol.* 33, 668.
- Krishna, R., Ellenberger, J., 1996. Gas holdup in bubble column reactors operating in the churn-turbulent flow regime. *AIChE J.* 42, 2627–2634.
- Kumar, S.B., 1994. Computed tomography measurements of void fraction and modeling of the flow in bubble columns. Ph.D. Thesis, Florida Atlantic University, Boca Raton, FL.
- Kumar, S.B., Moslemian, D., Dudukovic, M.P., 1995. A gamma ray tomographic scanner for imaging void fraction distribution in bubble columns. *Flow Meas. Instr.* 6, 61.
- Kumar, S.B., Moslemian, D., Dudukovic, M.P., 1997. Gas holdup measurements in bubble columns using computed tomography. *AIChE J.* 43, 1414–1425.
- Lin, T.-J., Tsuchiya, K., Fan, L.-S., 1998. Bubble flow characteristics in bubble columns at elevated pressure and temperature. *AIChE J.* 44, 545–560.
- Luo, X., Lee, D.J., Lau, R., Yang, G., Fan, L.S., 1999. Maximum stable bubble size and gas holdup in high-pressure slurry bubble columns. *AIChE J.* 42, 665–680.
- Oyevaar, M.H., De La Rie T., Der, S., Westerterp, K.R., 1989. Interfacial areas and gas holdups in bubble columns and packed bubble columns at elevated pressures. *Chem. Eng. Process.* 26, 1–14.
- Oyevaar, M.H., Westerterp, K.R., 1989. Mass transfer phenomena and hydrodynamics in agitated gas-liquid reactors and bubble columns at elevated pressures: state of the art. *Chem. Eng. Process.* 25, 85–98.
- Reilly, J.G., Scott, D.S., Bruijn, T., Jain, A., Diskorz, J., 1986. Correlation for gas holdup in turbulent coalescing bubble columns. *Can. J. Chem. Eng.* 64, 705.

- Shollenberger, K.A., Torczynski, J.R., Adkins, D.R., O'Hern, T.J., 1995. Bubble column measurements using gamma tomography. *ASME FED Fluid Measurement and Instrumentation* 211, 25–30.
- Shollenberger, K.A., Torczynski, J.R., Adkins, D.R., O'Hern, T.J., Jackson, N.B., 1997. Gamma-densitometry tomography of gas holdup spatial distribution in industrial-scale bubble columns. *Chem. Eng. Sci.* 52, 2037–2048.
- Sotelo, J.L., Benitez, F.J., Beltran-Heredia, J., Rodriguez, C., 1994. Gas holdup and mass transfer coefficients in bubble columns. I. porous glass-plate diffusers. *International Chem. Eng.* 34, 82–91.
- Wilkinson, P.M., Spek, A.P., Van Dierendonck, L.L., 1992. Design parameters estimation for scale-up of high-pressure bubble columns. *AIChE J.* 38, 544–554.
- Wilkinson, P.M., Dierendonck, L.L., 1990. Pressure and gas density effects on bubble break-up and gas hold-up in bubble columns. *Chem. Eng. Sci.* 45, 2309–2315.